

1 OKT. 1981

ARCHIEF

Lab. v. Scheepsbouwkunde
Technische Hogeschool
Delft

SHIPBUILDING

MARINE TECHNOLOGY MONTHLY

CONTENTS

INFLUENCE OF STARTING ACCELERATION AND
TOWROPE LENGTH ON TOWED BARGE TRAJEC-
TORY by R. Latorre and M.M. Bernitsas

*

A PRACTICAL CALCULATION METHOD OF SHIP
MANEUVERING MOTION by S. Inoue, M. Hirano,
K. Kijima and J. Takashina

*

VOLUME 28 - SEPTEMBER 1981 - No. 325

A PRACTICAL CALCULATION METHOD OF SHIP MANEUVERING MOTION

by

S. Inoue*, M. Hirano**, K. Kijima* and J. Takashina**

Summary

This paper presents a practical calculation method of the ship maneuvering motion using the principal particulars of ship hull, propeller and rudder as basic input data. The mathematical model, which describes the ship maneuvering motion, is developed employing the coupled equations of surge, sway, yaw, roll and propeller revolution. Computations are made for various kinds and types of the merchant ships and for wide range of the maneuvering characteristics. The computed results show satisfactory agreements with the full-scale trial results. In addition, as an application study, the effect of the loading condition on the ship maneuverability is investigated through the simulation calculations. The conclusion is that the calculation method of the present study is very useful and powerful for the predictions of the ship maneuverability at the time, such as the initial design stage etc., when the principal particulars of ship hull, propeller and rudder are known.

1. Introduction

Recent development of the maritime transportation has produced various types of ships, such as high-speed container carriers, roll-on/roll-off ships, pure car carriers and oil tankers from handy-sized product carriers to ULCCs. In relation to the problems of the maritime traffic safety, the diversification in ship types or the growth in ship sizes, mentioned above, has enhanced the significance of the maneuverability as one of the fundamental performances of ships. Namely it has become very important to predict precisely the ship maneuverability at the stage of the ship initial design. In addition, at the time of the ship completion, it has become necessary to provide the maneuvering informations for posting in the wheel house of ships, as is recommended by IMCO [1] and required by Panama Canal Regulations [2].

For these kinds of purposes, the simulation calculation technique of the maneuvering motion may be thought to be the most useful and powerful tool. Paying attention to this point, the authors have been making extensive efforts to develop a calculation method to simulate the ship maneuvering motion during the last several years [3], [4], [5], [6], [7]. In the previous report [8], estimate formulae of the hydrodynamic forces acting on ship hull in the maneuvering motion were presented, where the formulae were given as functions of the principal dimensions of ship hull. Succeeding the previous report [8], this report presents a practical calculation method of the ship maneuvering motion using the principal particulars of ship hull, propeller and rudder, which are usually known at the initial design stage, as basic input data.

The study in this report consists of three phases.

At first the mathematical model of the ship maneuvering motion is developed employing the coupled equations of surge, sway, yaw, roll and propeller revolution. Then computations are made for typical merchant ships covering various kinds and types of ships. Comparing the computed results with the results of the full-scale trials, the validity of the calculation method of the present study is examined for wide range of the maneuvering characteristics. In the last phase, an application study with the calculation method proposed in this report is made. The effect of the loading condition on the ship maneuverability is investigated through the simulation calculations taking three typical factors into consideration: the draft, the trim and the immersed rudder area, which are thought to affect the ship maneuverability in connection with the change of the loading condition.

The maneuvering motion treated in this report is that in calm and deep water condition, and the maneuvering motion with main engine operation such as the crash stop maneuver is not included here.

2. Mathematical model

2.1. Equations of motion

The ship maneuvering motion has generally been treated as the coupled motions in the horizontal plane, namely the coupled motions of surge, sway and yaw, assuming that the horizontal motions could be separated from other types of motion. In the derivation of the motion equations of this study, the following considerations are paid to the equations of the horizontal motions.

1. The coupling effect due to roll

Some ships such as high-speed container carriers and roll-on/roll-off ships perform considerable roll in

*) Faculty of Engineering, Kyushu University, Fukuoka, Japan.

**) Akishima Laboratory, Mitsui Engineering and Shipbuilding Co., Ltd., Tokyo, Japan.

their maneuvering motion. The recent study by the authors [9] reveals that the maneuvering motion of ships with large roll mentioned above should be calculated taking the coupling effect due to roll into consideration.

2. The coupling effect due to propeller revolution

In the maneuvering motion of full-scale ships the number of propeller revolution varies due to variation of both the propeller torque and the main engine torque even under the normal running condition of the main engine. This fact may suggest that the variation in the number of propeller revolution should be reflected in the calculation of the propeller thrust and the rudder forces. Namely it may be considered that the coupling effect due to propeller revolution on the horizontal motions can not be ignored.

A set of coordinate axes with origin fixed at the center of gravity of the ship (denoted with G hereinafter), as shown in Figures 1 and 2, is used to describe the ship maneuvering motion. Longitudinal and trans-

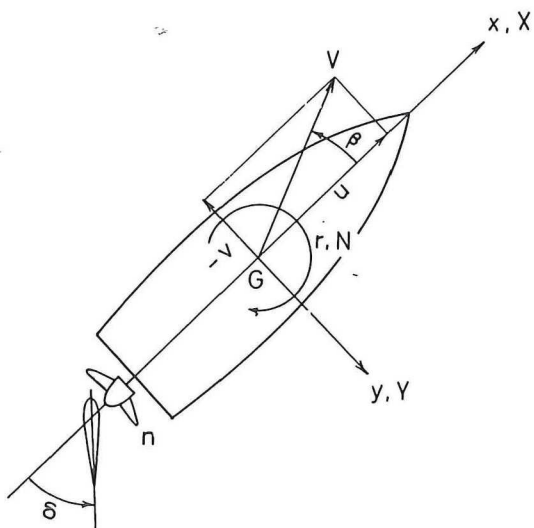


Figure 1. Coordinate system (1).

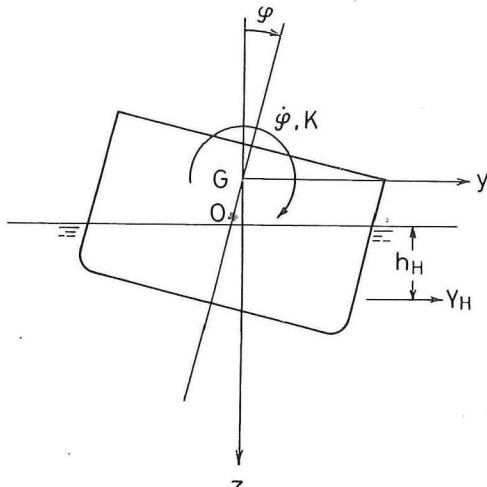


Figure 2. Coordinate system (2).

verse horizontal axes are represented by the x and y -axes respectively, and the z -axis is chosen so as to be perpendicular to the xy -plane (downward positive). By reference to this coordinate system G -xyz, the basic equations of the ship maneuvering motion can be written in the following form taking the coupling effects due to both roll and propeller revolution into consideration [6].

$$\begin{aligned} \text{Surge} &: m(\dot{u} - vr) = X_H + X_P + X_R \\ \text{Sway} &: m(\dot{v} + ur) = Y_H + Y_R \\ \text{Yaw} &: I_{zz}\dot{r} = N_H + N_R \\ \text{Roll} &: I_{xx}\ddot{\varphi} = K_H + K_R \end{aligned} \quad (1)$$

$$\text{Propeller revolution: } 2\pi J_{pp}\dot{n} = Q_E + Q_P$$

where the terms with subscript H represent the hydrodynamic forces produced by the motion of ship hull (without propeller and rudder) and acting on it, and the terms with subscript R represent the rudder forces including the hydrodynamic forces induced on ship hull by rudder action. The terms X_P , Q_P and Q_E in equation (1) represent the propeller thrust, the propeller torque and the main engine torque respectively.

2.2. Longitudinal force acting on ship hull, propeller thrust and propeller torque

The longitudinal force acting on ship hull X_H can be written

$$X_H = -m_x\dot{u} + (m_y + X_{vr})vr + X(u) . \quad (2)$$

The added inertia terms in equations (2) and (6), namely m_x , m_y and J_{zz} , can be estimated by making use of the estimate charts proposed by Prof. S. Motora [10]. Rewriting the coefficient of the second term in equation (2) as $m_y + X_{vr} = c_m m_y$, then c_m may have approximate value of $0.50 - 0.75$ [11]. The estimation of the second term can be made by giving an appropriate value to c_m . The third term in equation (2) represents ship resistance as a function of u .

The propeller thrust X_P and the propeller torque Q_P can be written

$$\begin{aligned} X_P &= (1 - t_{PO}) \cdot \rho n^2 D^4 K_T(J_P) \\ Q_P &= -2\pi J_{pp}\dot{n} - \rho n^2 D^5 K_Q(J_P) . \end{aligned} \quad (3)$$

The thrust coefficient $K_T(J_P)$ and the torque coefficient $K_Q(J_P)$ can be computed with the propeller characteristic curves as functions of the advance constant J_P , which is expressed as

$$J_P = u(1 - w_P)/(nD) . \quad (4)$$

The effective propeller wake fraction w_P , which is defined with the concept of the propeller thrust iden-

ity, may generally vary in the maneuvering motion from that in the straight running condition.

The following estimate formula is made based on some model experimental results [6].

$$w_P = w_{PO} \exp(K_1 \beta_P^2), K_1 = -4.0 \quad (5)$$

where the effect of the maneuvering motion on w_P is considered with the geometrical inflow angle at propeller position β_P , which is defined as $\beta_P = \beta - x'_P r'$.

2.3. Lateral force and yaw moment acting on ship hull

The lateral force and the yaw moment acting on ship hull, namely Y_H and N_H , can be written in the following form [6].

$$\begin{aligned} Y_H &= -m_y \dot{v} - m_x u r + Y_{H0}(v, r) + Y_{H1}(v, r, \varphi) \\ N_H &= -J_{zz} \dot{r} + N_{H0}(v, r) + N_{H1}(v, r, \varphi) \\ &\quad + [Y_{H0}(v, r) + Y_{H1}(v, r, \varphi)] x_s . \end{aligned} \quad (6)$$

The terms $Y_{H0}(v, r)$ and $N_{H0}(v, r)$ in equation (6) represent the fundamental force and moment which play an important part in the ship maneuvering motion. The authors have developed the estimate formulae of $Y_{H0}(v, r)$ and $N_{H0}(v, r)$, and the results have already been presented in detail in the previous report [8]. They are summarized briefly as follows. $Y_{H0}(v, r)$ and $N_{H0}(v, r)$ are expressed

$$\begin{aligned} Y_{H0}(v, r) &= \frac{1}{2} \rho L d V^2 [Y'_v v' + Y'_r r' + Y'_{v|r|} v' |v'| \\ &\quad + Y'_{v|r|} v' |r'| + Y'_{r|r|} r' |r'|] \\ N_{H0}(v, r) &= \frac{1}{2} \rho L^2 d V^2 [N'_v v' + N'_r r' + N'_{v|r|} v'^2 r' \\ &\quad + N'_{v|r|} v'^2 r' + N'_{r|r|} r' |r'|] . \end{aligned} \quad (7)$$

The derivatives in equation (7) can be estimated by knowing the principal dimensions of ship hull, namely L, B, d, C_B and τ . The estimate formulae for the linear derivatives are given in the form

$$\begin{aligned} Y'_v &= [a_1 k + f(C_B B/L)] (1 + b_1 \tau') \\ Y'_r &= a_2 k (1 + b_2 \tau') \\ N'_v &= a_3 k (1 + b_3 \tau') \\ N'_r &= (a_4 k + a_5 k^2) (1 + b_4 \tau') \end{aligned} \quad (8)$$

where

$$k = 2d/L, \tau' = \tau/d \quad (9)$$

and $a_1, a_2, \dots, b_1, b_2, \dots$ etc. are the constant. Estimate charts, as functions of the principal dimensions of ship hull, are given for the estimation of the nonlinear derivatives, where the effect of the trim is

not considered. It is advisable to refer to the report cited above [8] for the details of these charts.

The terms $Y_{H1}(v, r, \varphi)$ and $N_{H1}(v, r, \varphi)$ in equation (6) represent the added terms due to inclusion of the roll effect. According to the study by the authors [9], they can be written

$$\begin{aligned} Y_{H1}(v, r, \varphi) &= 0 \\ N_{H1}(v, r, \varphi) &= \frac{1}{2} \rho L^2 d V^2 [N'_\varphi + N'_{v|\varphi|} v' |\varphi| + \\ &\quad + N'_{r|\varphi|} r' |\varphi|] . \end{aligned} \quad (10)$$

The derivatives in equation (10) can be estimated by utilizing the results of the study cited above [9], namely

$$\begin{aligned} N'_\varphi &= c_1 \\ N'_{v|\varphi|} &= c_2 N'_v \\ N'_{r|\varphi|} &= c_3 N'_r \end{aligned} \quad (11)$$

where c_1, c_2 and c_3 are the constant.

2.4. Roll moment acting on ship hull

The roll moment acting on ship hull can be written

$$K_H = -J_{xx} \ddot{\varphi} - N(\dot{\varphi}) - W \cdot GZ(\varphi) - Y_H \cdot z_H . \quad (12)$$

The coupling effect due to the horizontal motions on the motion of roll is reflected in the form of $Y_H \cdot z_H$ in equation (12). As for the estimation of the vertical distance z_H (from G to the point on which Y_H acts), one of the authors has proposed an estimate chart [12], where estimate curves of $h_H (=z_H - OG)$ shown in Figure 2 are given as functions of C_B .

2.5. Rudder forces and moments

The rudder forces and moments including the hydrodynamic forces and moments induced on ship hull by rudder action, namely X_R, Y_R, N_R and K_R , can be written in the following form [6], [13].

$$\begin{aligned} X_R &= -F_N \sin \delta \\ Y_R &= -(1 + a_H) F_N \cos \delta \\ N_R &= -(1 + a_H) x_R F_N \cos \delta \\ K_R &= (1 + a_H) z_R F_N \cos \delta . \end{aligned} \quad (13)$$

In equation (13), the hydrodynamic force induced on ship hull by rudder action is described in the form of $a_H F_N \cos \delta$. The coefficient a_H can be estimated based on some model experimental results, which suggest that a_H may be expressed as a function of C_B [6]. The rudder normal force F_N can be written in the form

$$F_N = \frac{1}{2} \rho \frac{6.13 \lambda}{\lambda + 2.25} A_R V_R^2 \sin \alpha_R . \quad (14)$$

The effective rudder inflow speed and angle, namely V_R and α_R in equation (14), are calculated as follows [6].

1. The effective rudder inflow speed V_R

Introducing the effective rudder wake fraction w_R [11], which is defined with the concept of the rudder normal force identity, V_R can be expressed in the form

$$V_R = V(1 - w_R) [1 + K_2 g(s)]^{1/2} \quad (15)$$

where $K_2 = 1.065$ for the port rudder and $K_2 = 0.935$ for the starboard rudder. The term $K_2 g(s)$ in equation (15) represents the effect of the propeller slip-stream on V_R , and

$$g(s) = \eta \kappa [2 - (2 - \kappa)s] s/(1 - s)^2 \quad (16)$$

where

$$s = 1 - u(1 - w_P)/(nP) \quad (17)$$

$$\eta = D/H$$

$$\kappa = 0.6(1 - w_P)/(1 - w_R) .$$

The estimation of the effective rudder wake fraction is made assuming that w_R in the maneuvering motion could be computed by

$$w_R/w_{RO} = w_P/w_{PO} = \exp(K_1 \beta_P^2) . \quad (18)$$

The effective rudder wake fraction w_{RO} of full-scale ships may be obtained from the results of the model experiments in the same manner as for the effective propeller wake fraction w_{PO} in the area of the ship propulsion, namely making use of the technique to estimate the full-scale value from the model experimental results with the concept of the wake ratio.

2. The effective rudder inflow angle α_R

Taking the flow-rectifying effect into consideration, α_R can be expressed in the form

$$\alpha_R = \delta + \delta_O - \gamma \beta'_R \quad (19)$$

where β'_R is defined as $\beta'_R = \beta - 2x'_R r'$. The flow-rectifying effect may be considered to be constituted by two kinds of factors. One is the flow-rectifying effect due to ship hull and the other is due to propeller, then the flow-rectification coefficient γ can be written [14]

$$\gamma = C_P \cdot C_S . \quad (20)$$

The propeller flow-rectification coefficient C_P is given in the form

$$C_P = 1/[1 + 0.6\eta(2 - 1.4s)s/(1 - s)^2]^{1/2} . \quad (21)$$

The ship hull flow-rectification coefficient C_S is given in the following form based on some model experimental results [6]

$$\begin{aligned} C_S &= K_3 \beta'_R & \text{for } \beta'_R \leq C_{SO}/K_3 \\ C_S &= C_{SO} & \text{for } \beta'_R > C_{SO}/K_3 \end{aligned} \quad (22)$$

with $K_3 = 0.45$ and $C_{SO} = 0.5$.

2.6. Main engine torque

The types of the main engine treated here are the slow-speed diesel engine and the steam turbine, and the following torque characteristics are used.

1. The slow speed diesel engine

$$\begin{aligned} Q_E &= |Q_P| & \text{for } |Q_P| \leq Q_{EMAX} \\ Q_E &= Q_{EMAX} & \text{for } |Q_P| > Q_{EMAX} . \end{aligned} \quad (23)$$

2. The steam turbine

$$Q_E = SHP/(2\pi n) . \quad (24)$$

3. Numerical results

3.1. Full-scale maneuvering trials and ship selection

At the time of the ship completion, the full-scale sea trials for the maneuverability such as the turning test, Z-maneuver test etc. are conducted. In this report three kinds of the maneuvering tests, i.e. the turning test with 35° rudder, the $10^\circ - 10^\circ$ Z-maneuver test and the spiral test, are taken for the comparison purpose of the computed results with the results of the full-scale trials. Namely in order to examine the validity of the calculation method of the present study for wide range of the maneuvering characteristics, computations are made for the turning motion with 35° rudder, the $10^\circ - 10^\circ$ Z-maneuver and the spiral maneuver.

The ships, of which the comparisons are made, are selected so as to satisfy the following requirements.

1. The three kinds of the maneuvering tests mentioned above should have been conducted for each ship to be selected.
2. The full-scale maneuvering trials of each ship to be selected should have been conducted in the environmental condition below the 'slight' sea and below 5.0 m/sec wind speed.

Thus the following seven ships covering the various types and sizes of the merchant ships, namely from a general cargo boat of 10,000-DWT class to a ULCC, are selected from ships built in Mitsui Engineering and Shipbuilding Co., Ltd. during the last ten years.

- Ship A : high-speed container carrier
- Ship B : general cargo boat
- Ship C : roll-on/roll-off ship
- Ship D : pure car carrier
- Ship E : bulk carrier (70,000-DWT)
- Ship F : VLCC (270,000-DWT)
- Ship G : ULCC (370,000-DWT)

Table 1
Principal particulars of hull, propeller and rudder

ship	A	B	C	D	E	F	G
kind of ship	container carrier	cargo boat	ro/ro	pure car carrier	bulk carrier	VLCC	ULCC
loading condition	ballast	ballast	ballast	ballast	ballast	full	ballast
hull							
<i>L</i> (m)	202.00	160.00	212.00	180.00	230.00	318.00	348.00
<i>B</i> (m)	31.20	23.50	32.26	32.00	32.20	56.00	63.40
<i>d</i> (m)	6.93	5.20	6.29	6.80	7.24	20.58	9.64
τ (m)	1.95	3.78	1.13	1.03	1.05	0.0	3.95
C_B	0.518	0.600	0.612	0.566	0.820	0.827	0.788
rudder							
A_R/Ld	1/48.1	1/37.7	1/50.6	1/34.8	1/47.9	1/58.6	1/34.5
λ	1.40	1.57	1.22	1.19	1.38	1.55	1.28
propeller							
<i>D</i> (m)	7.10	5.70	6.60	6.20	6.70	8.90	9.60
<i>P/D</i>	1.04	1.14	0.97	0.95	0.71	0.71	0.71
<i>Z</i>	6	4	5	5	4	5	5

The principal particulars of ship hull, propeller and rudder of these ships are given in Table 1. The steam turbine is mounted as the main engine on ship F and ship G, and the slow-speed diesel engine on the other five ships.

3.2. Numerical results and comparisons with full-scale trial results

Computations based on the mathematical model described in chapter 2 are made for the three kinds of the maneuvering motions mentioned before, and the computed results are compared with the results of the full-scale trials as follows.

1. Turning motion with 35° rudder

The computed results of the turning motion with 35° rudder (the starboard turning) for all of the ships selected are shown with solid lines in the form of both the turning trajectory and the motion time-histories in Figures 3–18, where the results of the full-scale trials are also shown with empty circles. It can be mentioned from these figures that the computed results, with respect to both the turning trajectory and the time-histories of the heading angle, the ship speed and the number of propeller revolution, show satisfactory agreements with the results of the full-scale trials for all of the ships.

The coupling effect due to roll on the horizontal motions is examined for the turning motion of ship D, which performed large roll in her turning motion. (The maximum roll angle measured with clinometer in the

wheel house was about 10°). Computations are made also for the case without inclusion of the roll effect, and the results are shown with chain lines in Figures 9 and 10. It may be understood from Figures 9 and 10 that the computations without consideration of the roll effect give erroneous solutions, and that the maneuvering motion of a ship with large roll should be treated together with the motion of roll simultaneously. The authors have already confirmed this fact in the study with model experiments [9]. In this report the same fact is confirmed for the full-scale ship.

The coupling effect due to propeller revolution on the horizontal motions is examined for the turning motion of ship A. The computed results without inclusion of the propeller revolution effect are shown with chain lines in Figures 3 and 4, and poor agreements are seen between the computed and the full-scale trial results with respect to the time-histories of the heading angle and the ship speed. Hence it may be understood that the maneuvering motion of the full-scale ships should be calculated taking the coupling effect due to propeller revolution into consideration even under the normal running condition of the main engine.

Computations of ship F are made for both the full load condition and the ballast condition as shown in Figures 13–16. It can be recognized from these figures that the computed results with the calculation method of the present study explain well the differences of the motion time-histories between both loading conditions.

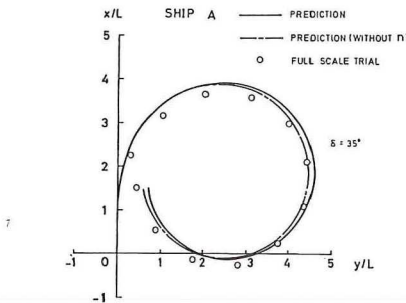


Figure 3. Turning trajectory (ship A).

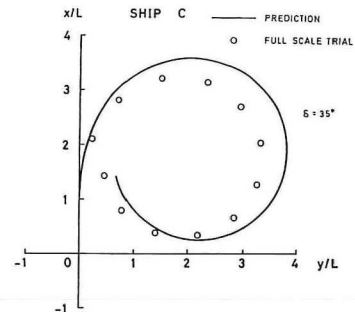


Figure 7. Turning trajectory (ship C).

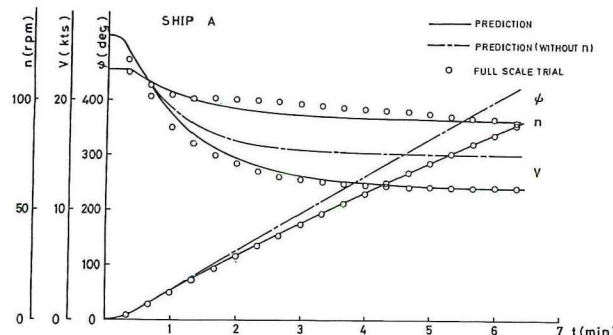


Figure 4. Time-histories of heading angle, ship speed and number of propeller revolution in turning motion (ship A).

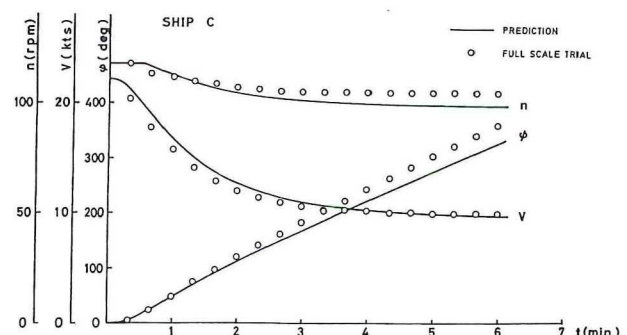


Figure 8. Time-histories of heading angle, ship speed and number of propeller revolution in turning motion (ship C).

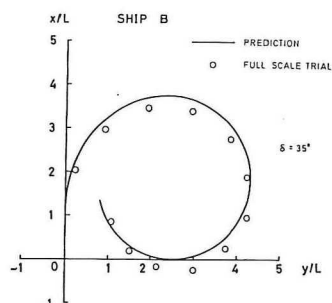


Figure 5. Turning trajectory (ship B).

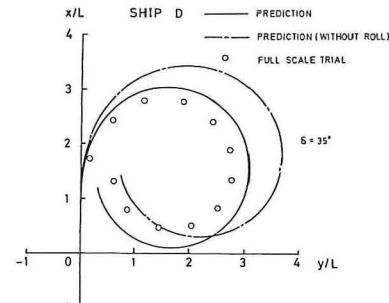


Figure 9. Turning trajectory (ship D).

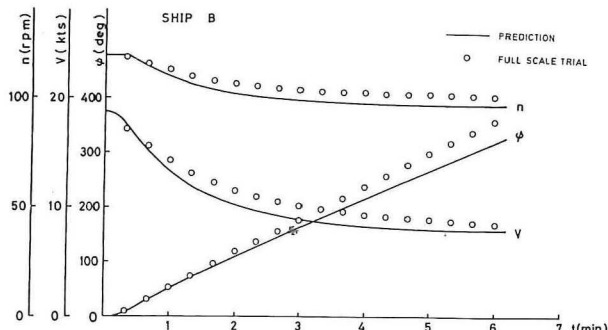


Figure 6. Time-histories of heading angle, ship speed and number of propeller revolution in turning motion (ship B).

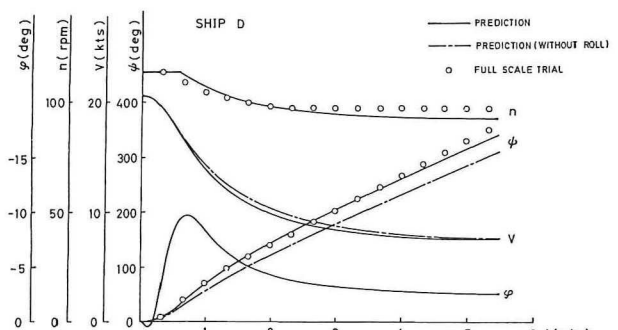


Figure 10. Time-histories of heading angle, ship speed, roll angle and number of propeller revolution in turning motion (ship D).

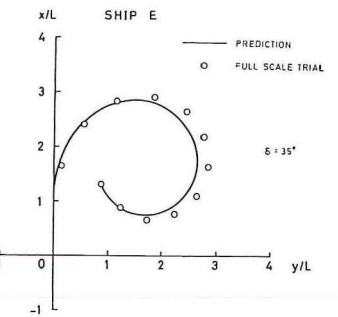


Figure 11. Turning trajectory (ship E).

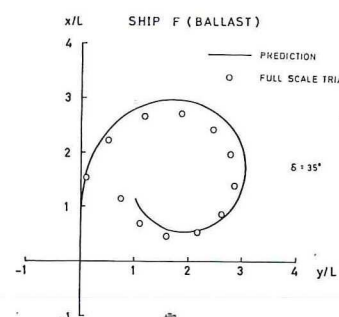


Figure 15. Turning trajectory (ship F ballast).

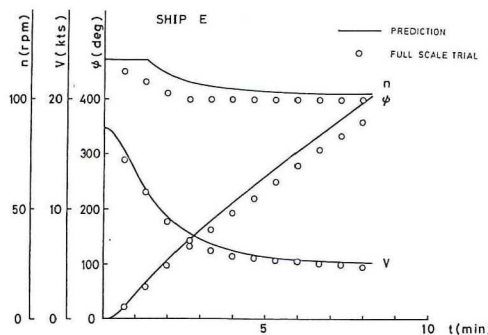


Figure 12. Time-histories of heading angle, ship speed and number of propeller revolution in turning motion (ship E).

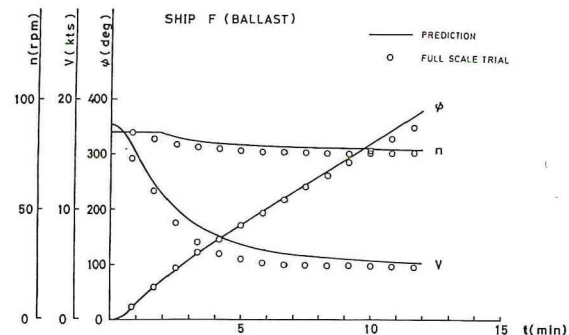


Figure 16. Time-histories of heading angle, ship speed and number of propeller revolution in turning motion (ship F ballast).

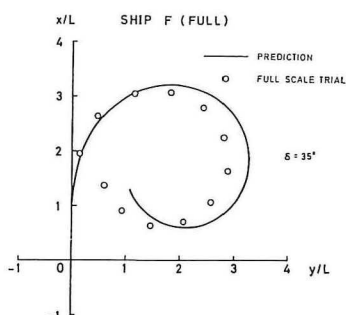


Figure 13. Turning trajectory (ship F full).

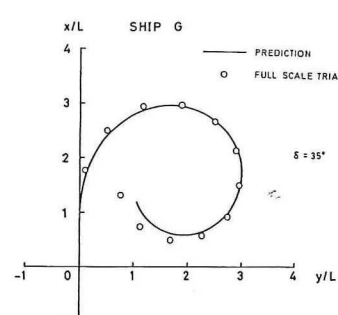


Figure 17. Turning trajectory (ship G).

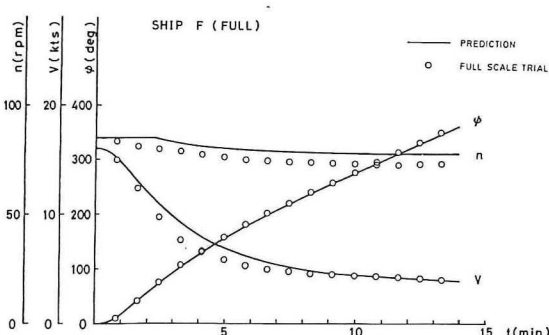


Figure 14. Time-histories of heading angle, ship speed and number of propeller revolution in turning motion (ship F full).

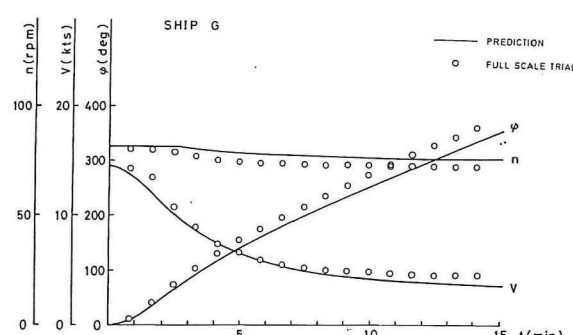


Figure 18. Time-histories of heading angle, ship speed and number of propeller revolution in turning motion (ship G).

2. $10^\circ - 10^\circ$ Z-maneuver

Computations of the $10^\circ - 10^\circ$ Z-maneuver are made for ship A, B, C, E and G, and the results are shown in the form of the time-histories of the heading angle and the ship speed (only for ship C and ship E) in Figures 19–23. Fairly good agreements between the computed and the full-scale trial results can be seen in these figures, especially with respect to the amplitude and the phase lag in the heading angle response.

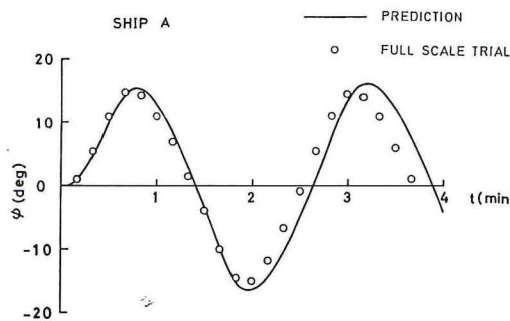


Figure 19. $10^\circ - 10^\circ$ Z-maneuver response (ship A).

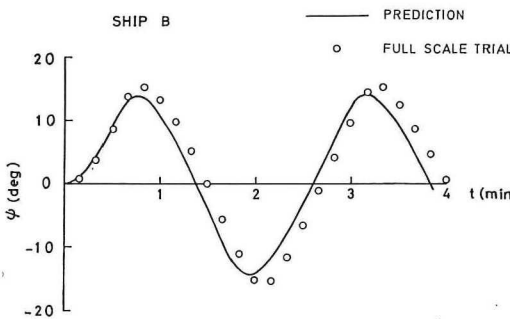


Figure 20. $10^\circ - 10^\circ$ Z-maneuver response (ship B).

3. Spiral maneuver

Computations of the spiral maneuver are made for ship A, B, C, E and F, where the reversed-spiral maneuver computations are added if necessary. The computed results are shown in the form of the steady turning performance in Figures 24–28. It can be mentioned from these figures that both the computed and the full-scale trial results are in fairly good agreements. Especially the computed results explain well the sensitive behavior of the steady turning performance of each ship in the region of small rudder angle.

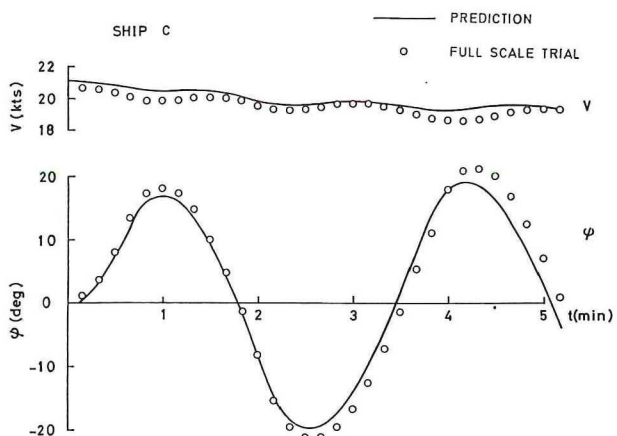


Figure 21. $10^\circ - 10^\circ$ Z-maneuver response (ship C).

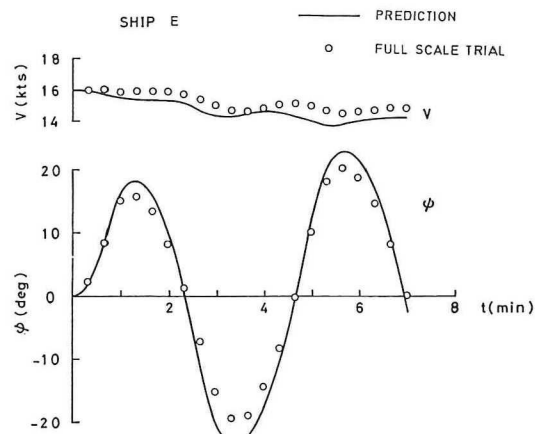


Figure 22. $10^\circ - 10^\circ$ Z-maneuver response (ship E).

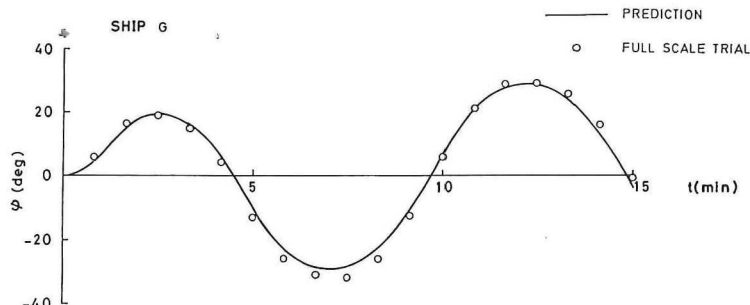


Figure 23. $10^\circ - 10^\circ$ Z-maneuver response (ship G).

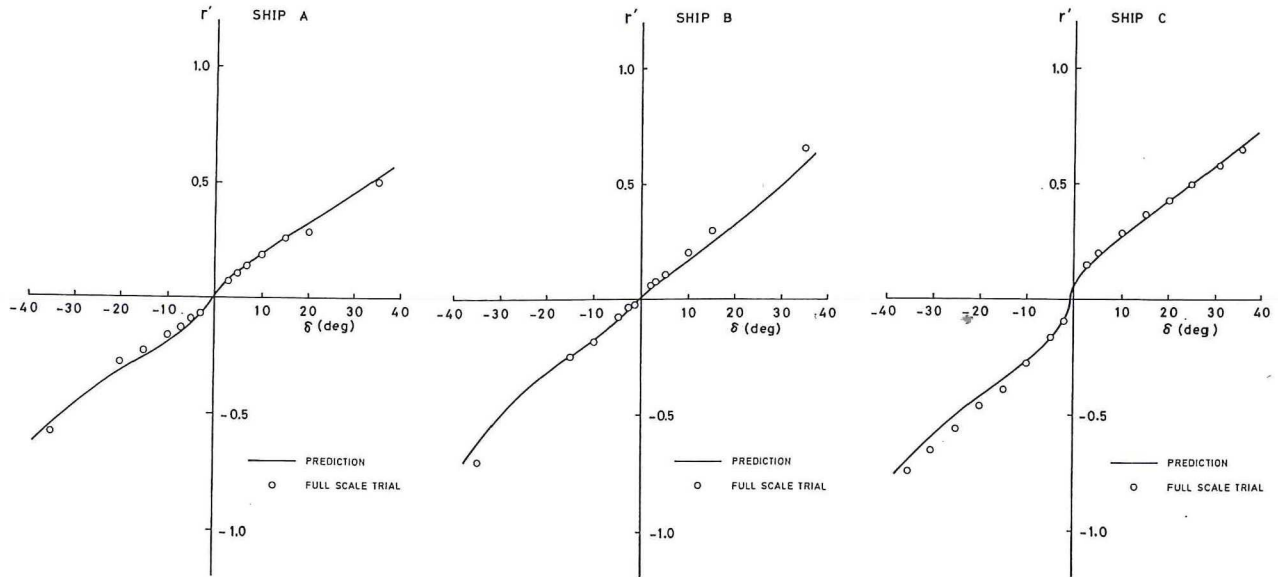


Figure 24. Steady turning performance (ship A).

Figure 25. Steady turning performance (ship B).

Figure 26. Steady turning performance (ship C).

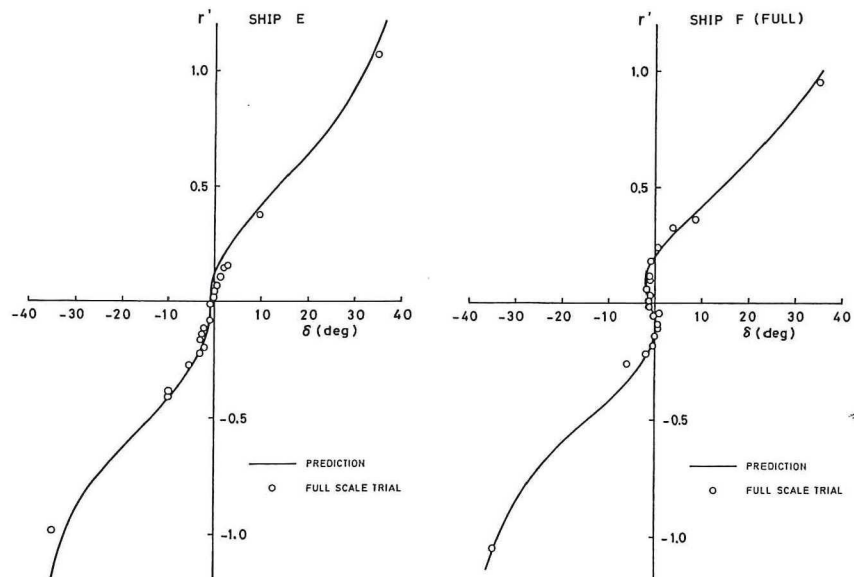


Figure 27. Steady turning performance (ship E).

Figure 28. Steady turning performance (ship F full).

4. Application study

4.1. Contents and procedure

As an application study with the calculation method proposed in the present study, the effect of the loading condition on the ship maneuverability is investigated through the simulation calculations. Two kinds of ships are selected for this purpose. One is a high-speed container carrier as a typical fine hull-form ship, and the other is a 230.000-DWT VLCC as a typical full hull-form ship. They are called as the container and the tanker respectively in this chapter. The principal particulars of ship hull, propeller and rudder of these ships are shown in Table 2.

Considering the factors which are thought to affect the ship maneuverability in connection with the change of the loading condition, the following three factors may be mentioned to be important: the draft, the trim and the immersed rudder area (defined in this report as the area of immersed part of rudder below still water surfaces) [7]. Rudder is completely immersed in water at the full load condition in general, and some upper part of rudder usually emerges above water surface at the ballast condition. By examining the effect of each factor mentioned above on the ship maneuverability, the investigations for the effect of the loading condition on the ship maneuverability

Table 2

Principal particulars of hull, propeller and rudder of full scale ship for simulation study

kind of ship loading condition	container		tanker	
	full	ballast	full	ballast
hull				
<i>L</i> (m)	202.00		310.00	
<i>B</i> (m)		31.20		54.00
<i>d</i> (m)	10.50	6.93	19.60	9.50
<i>W</i> (ton)	38,500	23,200	270,300	124,100
<i>r</i> (m)	0.0	2.02	0.0	3.10
<i>C_B</i>	0.566	0.518	0.803	0.761
rudder				
<i>A_R</i> / <i>Ld</i>	1/60.6	1/50.0	1/61.9	1/37.5
λ	1.67	1.35	1.51	1.17
propeller				
<i>D</i> (m)	7.10		7.90	
<i>P/D</i>	1.04		0.73	
<i>Z</i>	6		6	

are made. In Table 2, the trim and the immersed rudder area at the ballast condition are supposed to be 1.0 percent of the ship length (trim by stern) and to be 80 percent of the rudder area respectively for both ships. These figures are determined referring to those of both ships and similar ships in the full-scale trials.

In the process of the change of the loading condition, namely from the full load condition to the ballast condition, four kinds of conditions shown in Figure 29 are supposed.

1. FULL : The full load condition with zero trim and with fully immersed rudder.

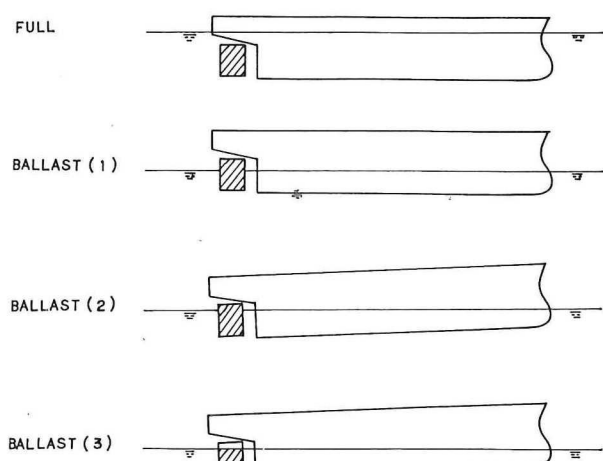


Figure 29. Concept of loading conditions for simulation study.

2. BALLAST (1) : An imaginary ballast condition with zero trim and with fully immersed rudder. (The draft is shallowed to the mean draft between fore- and aft-draft at the ballast condition).

3. BALLAST(2) : An imaginary ballast condition with fully immersed rudder.

4. BALLAST(3) : The ballast condition.

The above four conditions are thought out by changing the three factors, i.e. the draft, the trim and the immersed rudder area, one by one from the full load condition to the ballast condition. In this report the differences of the maneuverability between FULL and BALLAST(1), between BALLAST(1) and BALLAST(2), and between BALLAST(2) and BALLAST(3) are called as the draft effect, the trim effect, and the effect of the immersed rudder area respectively, where it should be noted that the draft effect includes the effect due to the change of the rudder area ratio (A_R/Ld) as well.

The transverse metacentric height GM usually changes considerably according to the change of the loading condition for such ships as the high-speed container carriers and roll-on/roll-off ships. Hence, in addition to the above-mentioned investigations, the effect of GM on the ship maneuverability is briefly examined in connection with the roll effect on the horizontal motions, although GM is somewhat different factor from the three factors taken above.

4.2. Numerical results and estimate formulae for loading condition effect

The effect of the loading condition on the ship maneuverability is investigated for the turning ability and the course changing ability, which are the typical features of the ship maneuverability. After these investigations the brief examination for the GM effect is added.

1. The turning ability

The four indices, i.e. the advance A_d (90° heading), the transfer T_r (90° heading), the tactical diameter D_t and the dimensionless turning rate r' (steady turning), are generally employed as the indices which represent the turning ability. The computed results of these indices for the four kinds of conditions are shown in Figure 30 for the container and in Figure 31 for the tanker, taking the rudder angle in abscissa. They are based on the results of the simulation calculations for the turning motion. The effect of the loading condition on A_d , T_r , D_t and r' can be understood from Figures 30 and 31 through the effect of each factor, i.e. the draft, the trim and the immersed rudder area, on them.

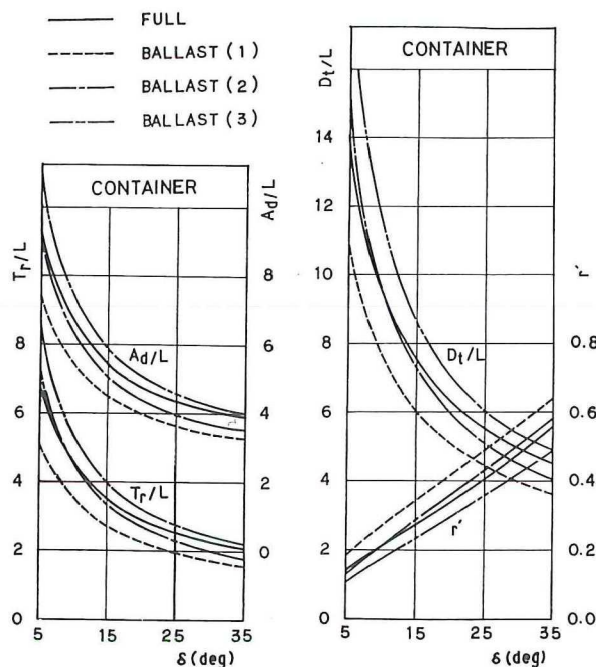


Figure 30. Computed results of advance, transfer, tactical diameter and dimensionless turning rate for the Container.

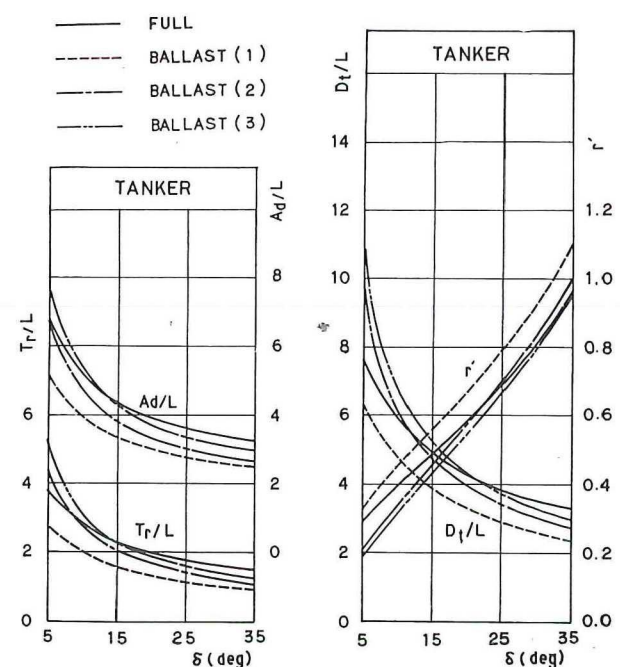


Figure 31. Computed results of advance, transfer, tactical diameter and dimensionless turning rate for the Tanker.

The full-scale maneuvering trials are usually conducted at one loading condition, namely either at the full load condition or at the ballast condition. It may be considered to be very useful if the estimation of the turning ability at a loading condition for which the full-scale trials are not conducted can be made by utilizing the full-scale trial results at the other loading condition. Hence an attempt is made to develop estimate formulae of the four indices which express the relations between the full load condition and the ballast condition with arbitrary draft, trim and immersed rudder area. The results obtained are written in the form

$$\begin{aligned}
 A_d(\text{Ballast}) &= (1 - A_1 d^*) (1 + B_1 \tau^*) \\
 &\quad (1 + C_1 a^*) \cdot A_d(\text{Full}) \\
 T_r(\text{Ballast}) &= (1 - A_2 d^*) (1 + B_2 \tau^*) \\
 &\quad (1 + C_2 a^*) \cdot T_r(\text{Full}) \\
 D_t(\text{Ballast}) &= (1 - A_3 d^*) (1 + B_3 \tau^*) \\
 &\quad (1 + C_3 a^*) \cdot D_t(\text{Full}) \\
 r'(\text{Ballast}) &= (1 + A_4 d^*) (1 - B_4 \tau^*) \\
 &\quad (1 - C_4 a^*) \cdot r'(\text{Full})
 \end{aligned} \tag{25}$$

where

$$\begin{aligned}
 d^* &= 1 - d_B/d_F \\
 \tau^* &= 100 \tau/L \\
 a^* &= 1 - A_R/A_{RO}
 \end{aligned} \tag{26}$$

The coefficients $A_1, A_2, \dots, B_1, \dots, C_1, \dots$ etc. in equation (25) can be determined based on the results shown in Figure 30 or Figure 31, and they are given in Figure 32 for both the container and the tanker.

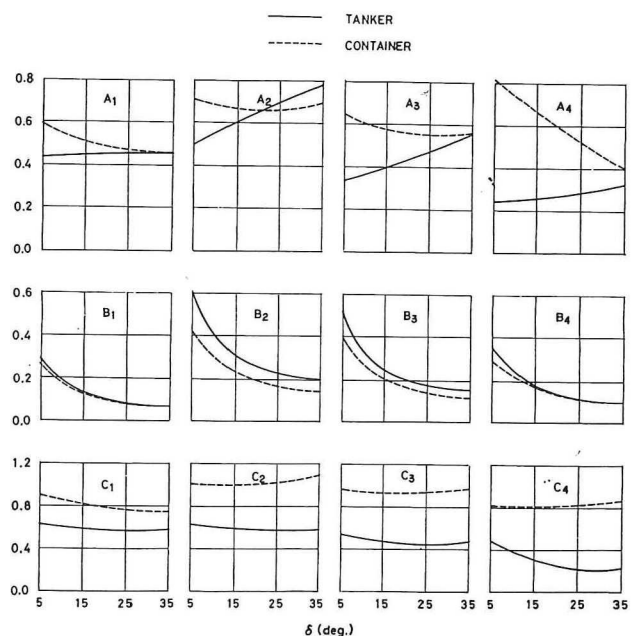


Figure 32. Coefficients A_1, A_2 etc. for indices of turning ability.

2. The course changing ability

At first the procedure of the $15^\circ/7^\circ$ course changing maneuver is briefly explained by making use of the figures shown in Figure 33. The rudder execution of

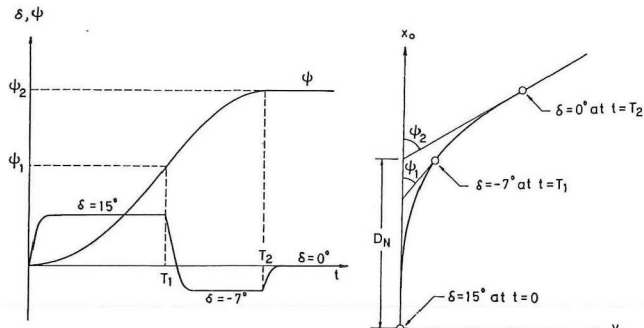


Figure 33. Illustration of course changing maneuver with rudder angle of $15^\circ/7^\circ$.

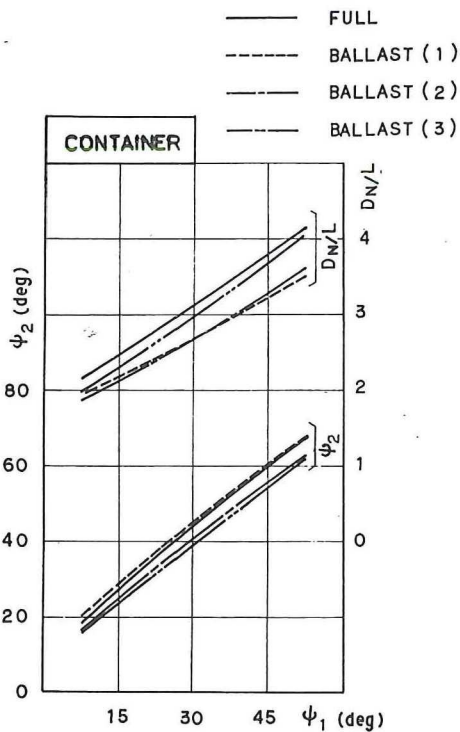


Figure 34. Computed results of new course distance and new course angle for the Container.

$\delta = 15^\circ$ is ordered at the time of $t = 0$, and the checking rudder with $\delta = -7^\circ$ is taken when the heading angle grows to $\psi = \psi_1$. The course changing maneuver is ended by returning the rudder amidship when the turning rate becomes zero. The heading angle at the end of the course changing maneuver, ψ_2 , is called as the new course angle, and the distance D_N shown in Figure 33 is called as the new course distance.

The course changing ability is generally discussed with the indices of ψ_2 and D_N . The computed results of these indices for the four kinds of conditions are shown in Figure 34 for the container and in Figure 35 for the tanker, taking the heading angle of ψ_1 in abscissa. They are based on the results of the simulation calculations for the $15^\circ/7^\circ$ course changing maneuver. The effect of the loading condition on ψ_2 and D_N can be understood from Figures 34 and 35.

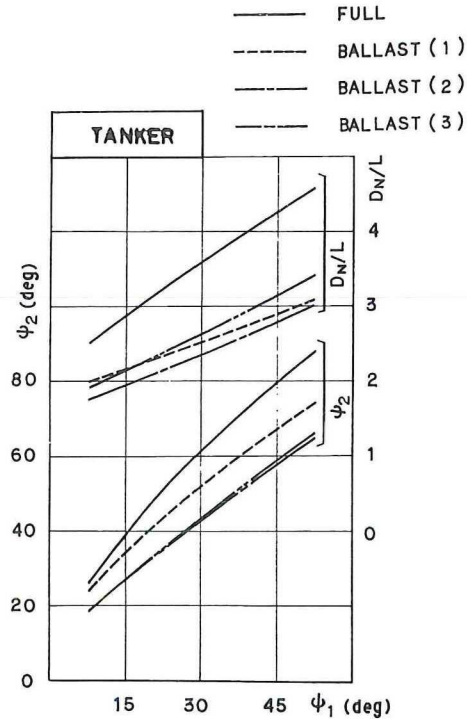


Figure 35. Computed results of new course distance and new course angle for the Tanker.

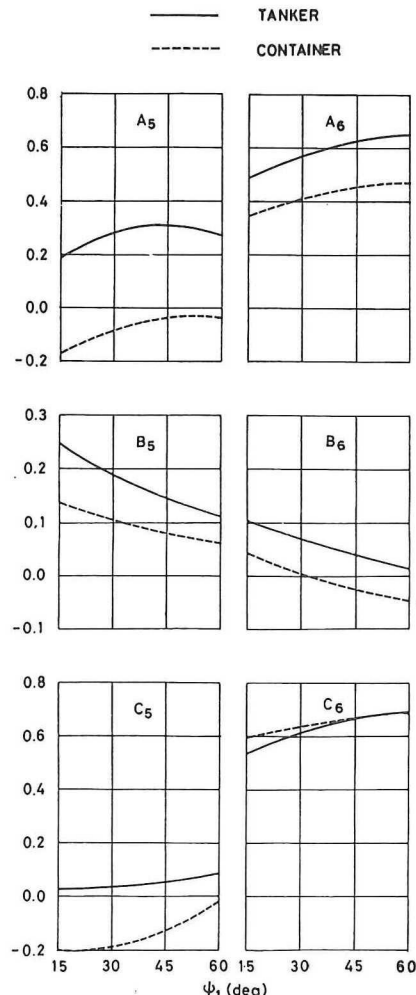


Figure 36. Coefficients A_5 , A_6 etc. for indices of course changing ability.

through the effect of each factor, i.e. the draft, the trim and the immersed rudder area, on them.

The same attempt as for the estimate formulae of the indices on the turning ability is made for the indices on the course changing ability. Namely the following expressions are obtained,

$$\begin{aligned}\psi_2(\text{Ballast}) &= (1 - A_5 d^*) (1 - B_5 \tau^*) \\ &\quad (1 + C_5 a^*) \cdot \psi_2(\text{Full}) \\ D_N(\text{Ballast}) &= (1 - A_6 d^*) (1 - B_6 \tau^*) \\ &\quad (1 + C_6 a^*) \cdot D_N(\text{Full})\end{aligned}\quad (27)$$

where the coefficients A_5 , A_6 , etc. in equation (27) can be determined based on the results shown in Figure 34 or Figure 35, and they are given in Figure 36 for both the container and the tanker.

3. The effect of GM

The GM effect is examined for the full load condition of the container. Computations are made for two cases of GM , i.e. $GM = \infty$ and $GM = 0.6\text{m}$. Figure 37 shows the computed results of the steady turning performance, and Figure 38 shows the computed results of the $10^\circ - 10^\circ$ Z-maneuver response. It can be recognized from these figures that the effect of GM on the maneuverability of ships such as the high-speed container carriers etc. can not be ignored in connection with the roll effect on the horizontal motions, and that the course keeping ability may be deteriorated in the case of small GM as is reported by Dr. H. Eda [15].

4.3. Comparisons with full-scale trial results

The validity of the results obtained through the simulation calculations for the effect of the loading

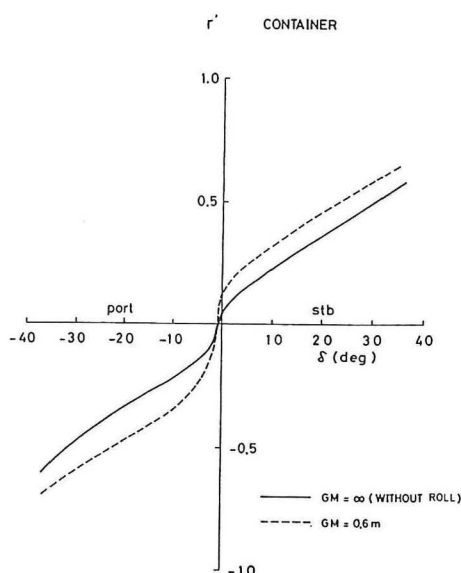


Figure 37. Computed results of steady turning performance for the Container.

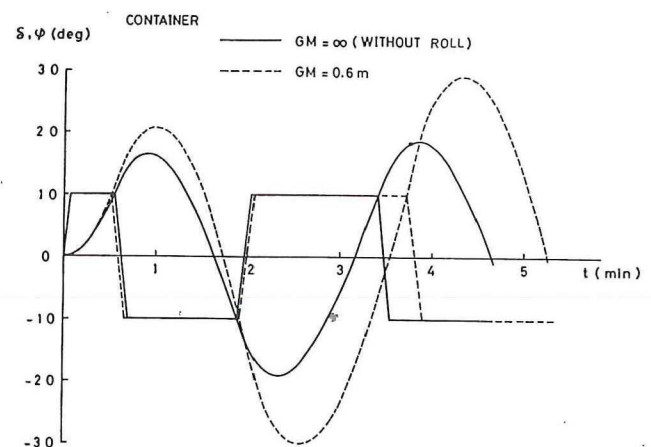


Figure 38. Computed results of $10^\circ - 10^\circ$ Z-maneuver response for the Container.

condition on the ship maneuverability is examined by comparing with the full-scale trial results.

1. The turning ability

The empty circles in Figure 39 show the full-scale trial results obtained in the turning test with 35° rudder of 200,000-DWT class VLCCs. The arrows in Figure 39 mean the estimation of the indices with equation (25) from the full load condition to the ballast condition, where as the value of the indices at the full load condition the mean values of the full-scale trial results are employed. It may be understood from Figure 39 that adequate results can be obtained by the estimate formulae of equation (25), although some scatter is seen in the full-scale trial results because the results of different hull-form ships from the tanker

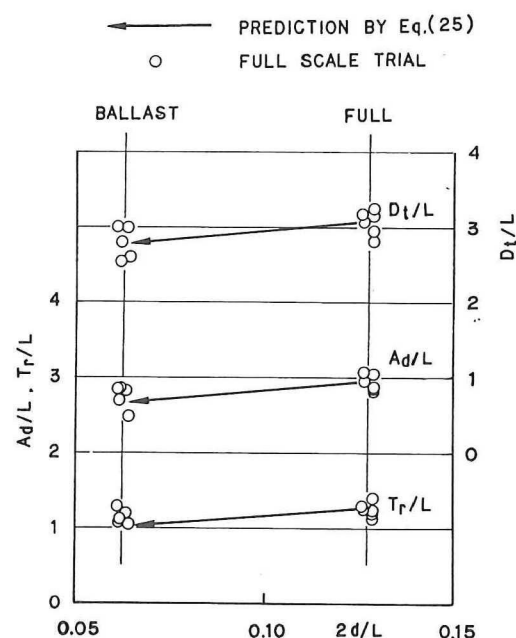


Figure 39. Comparison of predicted results of advance, transfer, and tactical diameter with those of full scale trial for the Tanker.

shown in Table 2 are included there. Both the computed and the full-scale trial results in Figure 39 indicate slight difference of the indices on the turning ability between the full load condition and the ballast condition, namely the indices in the latter condition are slightly smaller than those in the former condition. This may be due to the fact that the effect of each factor, i.e. the draft, the trim and the immersed rudder area, on the indices acts so as to cancel each other as a result, while the effect of each factor itself is not necessarily small as can be seen in Figures 30 and 31.

2. The course changing ability

Figures 40 and 41 show both the computed and the full-scale trial results for the indices on the course changing ability for the container and for the tanker respectively. The solid lines at the full load condition and at the ballast condition in Figure 40, which represent the computed results of the container, are the same ones as those at the FULL and at the BAL-LAST(3) in Figure 34 respectively. The same is explained for the computed results of the tanker shown in Figures 41 and 35. The results of different hull-form ships from the container or the tanker shown in Table 2 are added in the full-scale trial results, namely the results of different fine hull-form ships with C_B of 0.5 – 0.6 are added in Figure 40 and the results of different hull-form tankers and bulk carriers are added in Figure 41. It can be mentioned from Figures 40 and 41 that the results obtained through the simulation calculations for the course changing ability explain well the full-scale trial results, especially with respect to not only the effect of the loading condition but also the tendency with which the indices of ψ_2 and D_N vary according to the variation of ψ_1 .

5. Conclusions

It is the purpose of the present study to develop a practical calculation method of the ship maneuvering motion using the principal particulars of ship hull, propeller and rudder as basic input data. The computed results are compared with the results of the full-scale trials, and the validity of the calculation method of the present study is examined. In addition, as an application study, the effect of the loading condition on the ship maneuverability is investigated through the simulation calculations. The major results obtained in the study of this report are summarized as follows.

1. The computed results show satisfactory agreements with the results of the full-scale trials for various kinds and types of the merchant ships, namely from a general cargo boat of 10,000-DWT class to a ULCC, and for wide range of the maneuvering characteristics, namely for the turning motion with 35° rudder, the 10° – 10° Z-maneuver and the spiral maneuver.
2. The maneuvering motion of a ship with large roll should be treated together with the motion of roll simultaneously.
3. The maneuvering motion of the full-scale ships should be calculated taking the coupling effect due to propeller revolution into consideration even under the normal running condition of the main engine.
4. The effect of the loading condition on the ship maneuverability is investigated and clarified by examining the effects of three typical factors: the draft, the trim and the immersed rudder area, which are thought to affect the ship maneuverability in connection with the change of the loading condition.

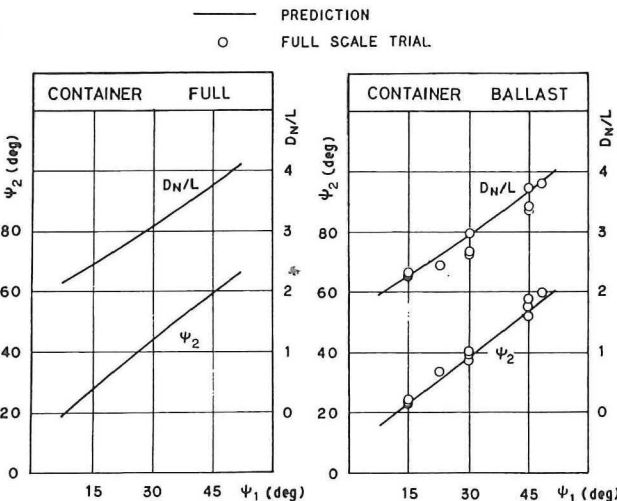


Figure 40. Comparison of predicted results of new course distance and new course angle with those of full scale trials for the Container.

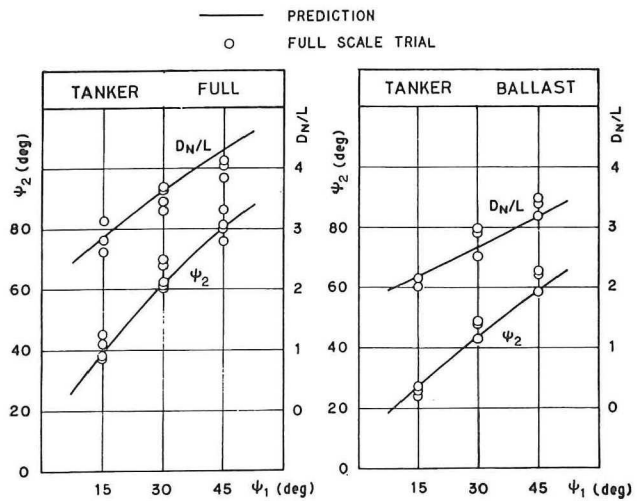


Figure 41. Comparison of predicted results of new course distance and new course angle with those of full scale trials for the Tanker.

5. The estimate formulae of equations (25) and (27) are useful for the estimations of the turning ability and the course changing ability at a loading condition, for which the full-scale trials are not conducted, when the full-scale trial results at the other loading condition are available.
6. Finally the calculation method of the present study is very useful and powerful for the predictions of the ship maneuverability at the time, such as the initial design stage etc., when the principal particulars of ship hull, propeller and rudder are known.

References

- IMCO: Recommendation on information to be included in the manoeuvring booklets, Resolution A. 209 (VII) adopted on 12 October 1971.
- Maneuvering characteristics: Data required, Code of Federal Regulations, 35 Panama Canal par. 103, 41a, 1977.
- Inoue, S., Hirano, M., Hirakawa, Y. and Mukai, K., 'The hydrodynamic derivatives on ship maneuverability in even keel condition' (in Japanese), Transactions of the West-Japan Society of Naval Architects, No. 57, 1979.
- Inoue, S., Hirano, M. and Mukai, K., 'The non-linear terms of lateral force and moment acting on ship hull in the case of maneuvering' (in Japanese), Transactions of the West-Japan Society of Naval Architects, No. 58, 1979.
- Inoue, S., Kijima, K. and Moriyama, F., 'Presumption of hydrodynamic derivatives on ship maneuvering in trimmed condition' (in Japanese), Transactions of the West-Japan Society of Naval Architects, No. 55, 1978.
- Hirano, M., 'On the calculation method of ship maneuvering motion at the initial design phase' (in Japanese), Journal of the Society of Naval Architects of Japan, Vol. 147, 1980.
- Inoue, S., Hirano, M., Kijima, K. and Takashina, J., 'An application of simulation study of maneuvering motion' (in Japanese), Transactions of the West-Japan Society of Naval Architects, No. 61, 1981.
- Inoue, S., Hirano, M. and Kijima, K., 'Hydrodynamic derivatives on ship maneuvering', International Shipbuilding Progress, Vol. 28, No. 321, 1981.
- Hirano, M. and Takashina, J., 'A calculation of ship turning motion taking coupling effect due to heel into consideration', Transactions of the West-Japan Society of Naval Architects, No. 59, 1980.
- Motora, S., 'On the measurement of added mass and added moment of inertia for ship motions (Part 1, 2 and 3)' (in Japanese), Journal of the Society of Naval Architects of Japan, Vol. 105 and 106, 1959 and 1960.
- Yoshimura, Y. and Nomoto, K., 'Modeling of maneuvering behaviour of ships with a propeller idling, boosting and reversing' (in Japanese), Journal of the Society of Naval Architects of Japan, Vol. 144, 1978.
- Inoue, S., 'On the point in vertical direction on which lateral force acts' (in Japanese), Technical Report, SP 82, Technical Committee of the West-Japan Society of Naval Architects, 1979.
- Ogawa, A. and Kasai, H., 'On the mathematical model of maneuvering motion of ships', International Shipbuilding Progress, Vol. 25, No. 292, 1978.
- Yumuro, A., 'Some experiments on flow-straightening effect of a propeller in oblique flows' (in Japanese), Journal of the Society of Naval Architects of Japan, Vol. 145, 1979.
- Eda, H., 'Rolling and steering performance of high speed ships', 13th Symposium on Naval Hydrodynamics, 1980.

Nomenclature

A_d	advance	I_{xx}, I_{zz}	moment of inertia of ship with respect to x and z -axes respectively
A_R	rudder area (immersed part below still water surface)	I_{pp}	moment of rotary inertia of propeller-shafting system
A_{RO}	rudder area	J_{xx}, J_{zz}	added moment of inertia of ship with respect to x and z -axes respectively
a_H	ratio of hydrodynamic force, induced on ship hull by rudder action, to rudder force	J_{pp}	added moment of rotary inertia of propeller
B	breadth of ship	L	length of ship (between perpendiculars)
C_B	block coefficient	m	mass of ship
C_P	propeller flow-rectification coefficient	m_x, m_y	added mass of ship in x and y -axes direction respectively
C_S	ship hull flow-rectification coefficient	$N(\dot{\varphi})$	roll damping moment
D	propeller diameter	n	number of propeller revolution
D_N	new course distance	P	propeller pitch
D_t	tactical diameter	r	turning rate
d	draft of ship (mean draft)	r'	dimensionless turning rate ($= rL/V$)
d_B	draft at ballast condition (mean draft)	T_r	transfer
d_F	draft at full load condition	t_{PO}	thrust deduction coefficient in straight running condition
F_N	rudder normal force	u	ship speed in x -axis direction
$GZ(\varphi)$	restoring moment lever of roll	V	ship speed ($= (u^2 + v^2)^{1/2}$)
H	rudder height	V_R	effective rudder inflow speed
h_H	vertical distance from still water surface to point on which lateral force Y_H acts (see Figure 2)		

v	ship speed in y -axis direction	x_a	x -coordinate of midship
v'	dimensionless ship speed in y -axis direction $(= v/V)$	z_H	z -coordinate of point on which lateral force Y_H acts
W	displacement of ship	z_R	z -coordinate of point on which rudder force Y_R acts
w_p	effective propeller wake fraction	α_R	effective rudder inflow angle
w_{PO}	effective propeller wake fraction in straight running condition	β	drift angle ($= -\sin^{-1} v'$)
w_R	effective rudder wake fraction	γ	flow-rectification coefficient
w_{RO}	effective rudder wake fraction in straight running condition	δ	rudder angle
x_p	x -coordinate of propeller position	λ	aspect ratio of rudder
x'_p	dimensionless form of x_p ($= x_p/L$)	ρ	density of water
x_R	x -coordinate of point on which rudder force Y_R acts	τ	trim quantity
x'_R	dimensionless form of x_R ($= x_R/L$)	φ	roll angle
		ψ	heading angle
		ψ_2	new course angle